JTTEE5 24:836–847
DOI: 10.1007/s11666-015-0246-y
1059-9630/$19.00 © ASM International

Beneficial Effects of Synchronous Laser Irradiation on the Characteristics of Cold-Sprayed Copper Coatings

Bo Li, Lijing Yang, Zhihong Li, Jianhua Yao, Qunli Zhang, Zhijun Chen, Gang Dong, and Liang Wang

(Submitted November 3, 2014; in revised form January 24, 2015)

Cold spray (CS) is an emerging materials deposition technique in which metallic particles are accelerated to a high velocity in a supersonic gas flow and then impinged onto a substrate to form a coating at a temperature well below the melting point of sprayed materials. The coating microstructure and properties are greatly influenced by particle preheating and substrate softening. This article presents a study of CS process of copper powder, with assistance of synchronous laser irradiation. The influence of synchronous laser irradiation on the Cu coating characteristics was investigated. The results show that the coating surface with laser irradiation is smoother than that without laser irradiation. The peak coating thickness is increased by about 70% as synchronous laser irradiation is employed, indicating an improvement in deposition efficiency. It is also found that with synchronous laser irradiation the coating is denser and the coating-substrate interfacial bonding is better as compared with that without laser irradiation. Moreover, the EDS and XRD analyses find Cu oxidation occurrence in the SLD coating, but the oxide is trivial. The aforementioned improvements on the coating largely arise from particle preheating and substrate softening by synchronous laser irradiation in the CS process.

Keywords cold spray, deposition efficiency, interfacial bonding, microhardness, synchronous laser irradiation

1. Introduction

Cold spray (CS) is a relatively new materials deposition technique whereby metal powders ranging in particle size from 5 to 100 μm are accelerated to a high velocity in a supersonic gas flow and then impinge onto the substrate or already deposited coating at a temperature well below the melting point of sprayed materials (Ref 1-3). Intensive plastic deformation induced by the high-velocity impact occurs in solid-state particle, substrate (or already deposited coating) or both, enabling the formation of a less-oxidized cold-sprayed coating. In the past few years, a wide range of pure metals, metallic alloys, polymers, and composites have been successfully deposited onto a variety of substrate materials using CS process (Ref 4-11).

One of the most widely used concepts in CS process is the critical velocity which is material-dependent (Ref 12). The critical velocity for a given powder is the velocity that an individual particle must achieve in order to effectively deposit after impact with substrate. Small particles more easily achieve high velocities than large particles. Since powders generally contain a mixture of particles with various sizes, some fraction of the powder is deposited on the substrate while the remainder bounces off. The ratio of the weight of powder deposited onto the substrate to that of the total powder used is called the deposition efficiency. It is evident that this ratio can be increased by reducing the critical velocity and/or increasing the impact velocity. The particle velocity in CS is affected by several factors such as gas condition, particle characteristics, nozzle geometry, etc. To improve the deposition efficiency of cold spray, considerable research has been made to investigate the effects of these factors on the coating formation (Ref 13-15).

Fukumoto et al. (Ref 16) pointed out that high gas temperature and long spraying time can increase the substrate temperature, thus improving the deposition efficiency. Legoux et al. (Ref 17) found that substrate preheating elevated the substrate temperature, which benefited the particle deformation and coating formation. The work of King et al. (Ref 18) further confirmed that substrate preheating promoted the occurrence of interfacial melting and hence the bonding between the particles and substrate. In addition to substrate preheating, particle temperature also influences the particle deposition significantly. Assadi et al. (Ref 19) predicted that the critical velocity can reduce by 40 m/s for a 100 °C increase in the particle temperature using analytical simulation, which took into consideration the particle temperature in the determination of a critical particle velocity. Lee et al. (Ref 20) showed experimentally that the critical velocity

Bo Li, Lijing Yang, Zhihong Li, Jianhua Yao, Qunli Zhang, Zhijun Chen, Gang Dong, and **Liang Wang**, Research Center of Laser Processing Technology and Engineering, Zhejiang University of Technology, Hangzhou 310014, P.R. China and Collaborative Innovation Center of High-end Laser Manufacturing Equipment, Hangzhou 310014, Zhejiang P.R. China. Contact e-mails: libo1011@zjut.edu.cn and laser@zjut.edu.cn.

was decreased by 50 m/s as the process gas temperature was increased by 100 °C.

From the above-mentioned studies, it can be concluded that an increase in particle and/or substrate temperature can enhance deposition efficiency and also reduce the critical deposition velocity as a result of softening effect. Moreover, increased substrate temperature may also help to promote the interface bonding of the coatings, since CS coatings generally have lower bonding strength than those produced by other deposition processes because of the short interaction time between the particles and the substrate (Ref 19). However, it has also been noted that elevating particle temperature by raising gas temperature increases the risk of nozzle fouling when spraying low melting point metals. As a result, a method of simultaneous heating of the particles and substrate without clogging the Laval nozzle would be desired.

Recently, O'Neill et al. developed supersonic laser deposition (SLD) by introducing laser into CS process (Ref 21, 22). In SLD, the deposition site of CS is simultaneously heated by laser in order to preheat particles and soften substrate as well. This method of heating the particle not only avoids nozzle fouling but also significantly reduces the critical velocity, which allows bonding to occur upon impact at the velocity about half that in cold spray.

In this study, the CS process of copper powder was assisted with synchronous laser irradiation, in order to preheat the particle and soften the substrate simultaneously. The effects of synchronous laser irradiation on the coating characteristics such as coating surface morphology, thickness, density, interfacial bonding, oxidation, and microhardness were investigated and elucidated by comparing the Cu coatings prepared by CS and SLD, respectively.

2. Experimental Section

2.1 Materials

Commercially available pure Cu powder (99.72%, Shanghai CNPC Powder Material Co. Ltd., Shanghai, P.R. China) was used as received. Figure 1(a) shows the irregular morphology of the Cu powder, although a few spherical particles were also observed. The powder size distribution was determined by the laser diffraction particle size analyzer (Horiba LA-950, Japan). The diameter distribution of the Cu powder is presented in Fig. 1(b) and it has a mean particle size of 25 μm. The substrate material is carbon with chemical composition listed in Table 1. The experimental specimen has a dimension of 100 × 60 × 10 mm with thickness of 10 mm. Before the coating process, the substrate surface was grit-blasted using 24 mesh alumina and ultrasonically cleaned in alcohol.

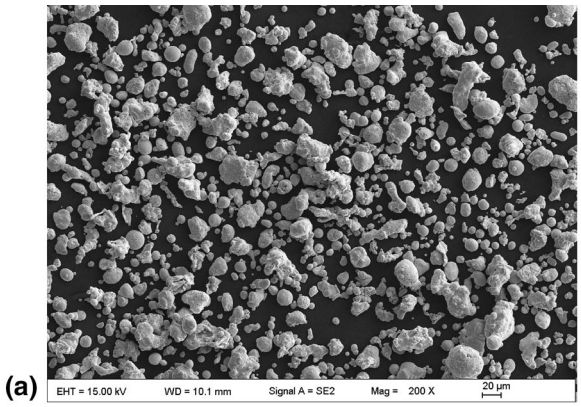

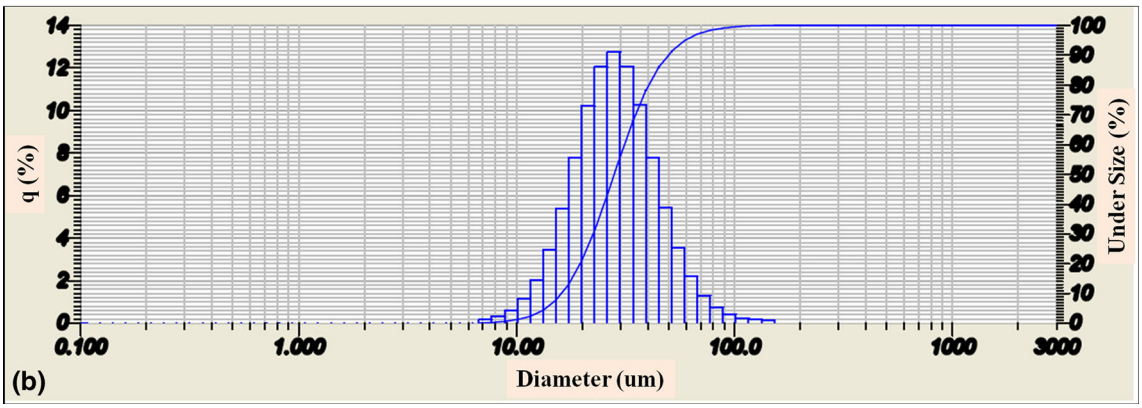

Fig. 1 SEM image (a) and powder size distribution (b) of Cu feedstock

2.2 Supersonic Laser Deposition (SLD) System

The schematic diagram of the SLD system used in this study is shown in Fig. 2, which was composed of CS system, laser unit, high pressure gas supply unit, and other auxiliary equipment like robot. High pressure air about 10-35 bar was supplied to a converging-diverging nozzle in two directions; one was through the gas heater, the other was via a powder feeder where Cu powder was held. The Cu feedstock stream and air were mixed and passed through the nozzle where the Cu particles were accelerated to supersonic speed. The high-velocity particles impacted a region of the substrate which was synchronously heated by a diode laser with 960-980 nm wavelengths and 4 kW maximum power (Laserline LDF 400-1000, Germany). Combined lenses were used to focus the laser beam onto the substrate surface and the diameter of the laser spot was 5 mm on the substrate surface. Laser power was controlled by a feedback system which utilized an infra-red pyrometer to monitor deposition zone temperature. Temperature control precision of the pyrometer was about ±2 °C. The nozzle, laser head, and pyrometer were installed on a robot (STAÜBLI TX 90, Switzerland). The CS system was designed and made by the Chinese Academy of Sciences. An in-house made de Laval nozzle with an area expansion ratio of ~8.3 and a length of 180 mm was used.

Table 1 Chemical composition of substrate material

Elements	C	Si	Mn	P	S	Fe
Wt.%	0.43	0.23	0.66	0.002	0.014	Bal.

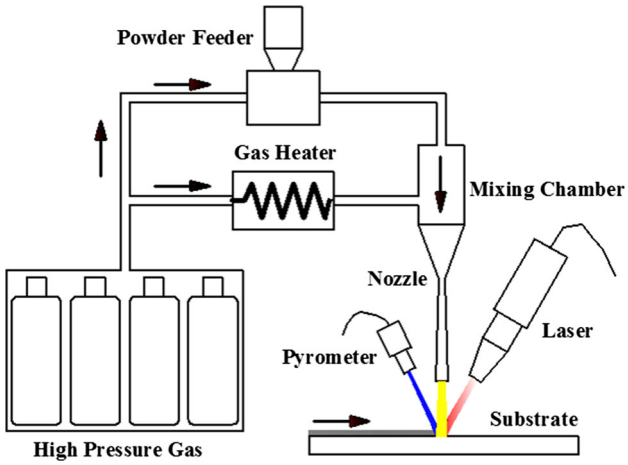

Fig. 2 Schematic diagram of SLD system

2.3 Coating Fabrication

The Cu coatings were produced using the above-SLD system. In the deposition process, the substrate was stationary and the nozzle, laser head, and pyrometer were moveable, controlled by the robot. As shown in Fig. 2, the spraying nozzle was perpendicular to the substrate surface and the laser beam was at an angle of 30° to the surface normal. The powder stream and the laser beam partially overlapped with each other. Therefore, during the coating process the impinging particles were also partially irradiated by the laser beam prior to hitting the substrate. The working gas was air. The Cu coatings were deposited under a wide range of process parameters such as gas pressure, gas temperature, laser power, laser traverse speed (also robot traverse speed), powder feeding rate, and standoff distance, in order to obtain the optimal deposition condition. The optimized parameters were obtained by taking into consideration coating surface morphology, coating thickness, coating density, interfacial bonding, coating oxidation, and coating hardness, which are shown in Table 2. In SLD process, the laser power was elaborately controlled to only soften both the spraying particles and substrate surface, not melting them. For comparison the cold-sprayed Cu coating was prepared under the same condition except that laser irradiation was not involved.

2.4 Coating Characterization

The phase structure of the Cu feedstock powder and as-deposited coatings were analyzed by X-ray diffractometer (XRD, D8 Advance, Brucker) using Cu-Ka radiation, 45 kV, 40 mA, and a scan rate of 0.02°/s. The cross-section microstructures and element distribution of the coatings were analyzed with scanning electron microscope (SEM, ΣIGMA HV-01-043, Carl Zeiss) and energy dispersive spectrometer (EDS, Nano Xflash Detector 5010, Bruker). The coating surface profile was characterized by a three-dimensional laser microscopy (LEXT OLS4100, OLYMPUS). The microhardness of the coatings was studied using a Vickers Indenter (HR-150DT, DHT), with 12 points tested on each sample (from coating surface to coating/substrate interface). The distance between the neighboring tested points was 0.1 mm. The weight and the duration used for each hardness measurement were 10 g and 10 s, respectively.

2.5 Modeling Description

The impact behavior of Cu particle on carbon steel substrate was simulated using the software package ANSYS Multiphysics/LS-DYNA. Owing to the axisymmetric characteristic of normal impact process, a 3D quarter model of single particle impact on substrate was

Table 2 Optimized process parameters for SLD-Cu coating

Gas pressure	Gas temperature	Laser power	Laser traverse speed	Powder feeding rate	Standoff distance
2.4 MPa	400 °C	800	10 mm/s	40 g/min	30 mm

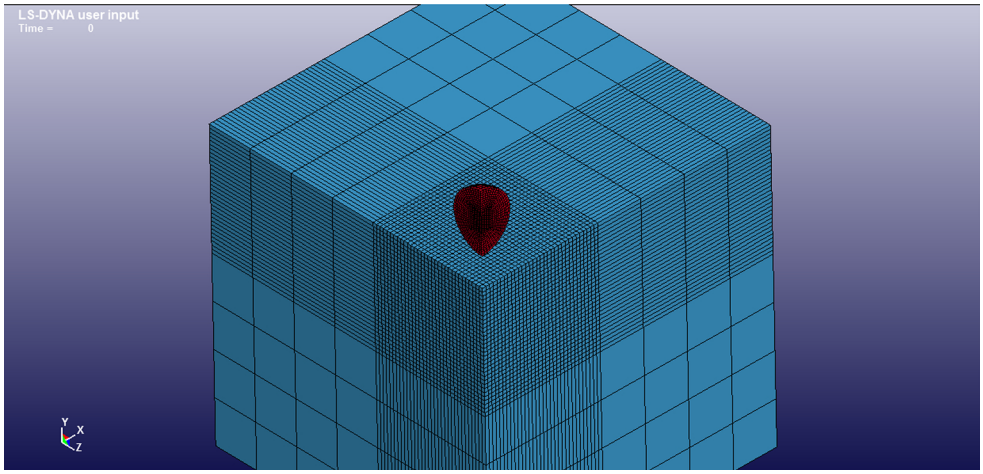

Fig. 3 Simulation model of Cu particle impacting onto steel substrate

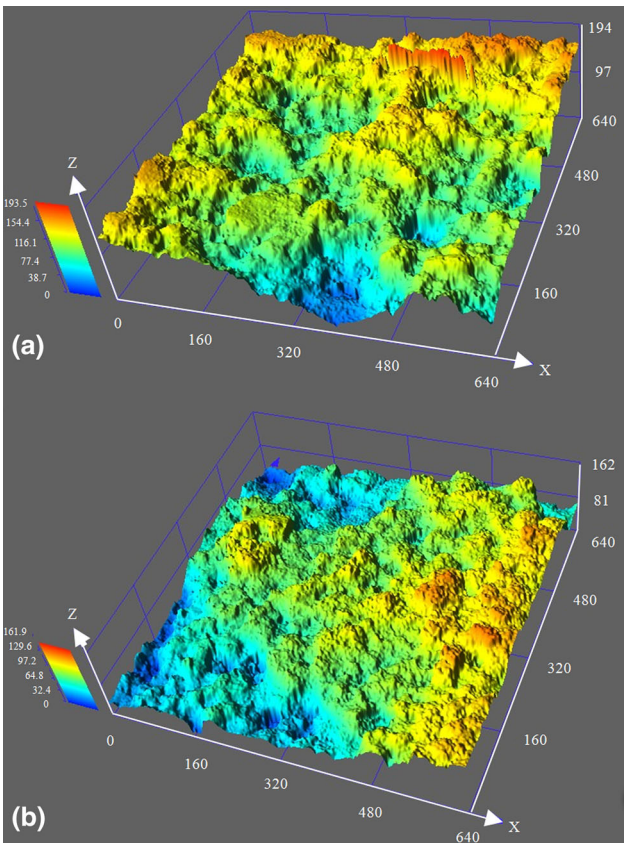

Fig. 4 Three-dimensional (3D) profile of surface morphology (a) CS-Cu, (b) SLD-Cu

simulated with Lagrangian formulation as shown in Fig. 3. The meshing was conducted using 3D Eulerian eight-node elements with a mesh size of 0.2 μm.

The material flow behavior of the Cu particle and steel substrate is described by the Johnson-Cook plasticity model, which has been widely used for CS simulation (Ref 23, 24). In the present model, the particle/substrate impact process was assumed to be an adiabatic process according to literatures (Ref 19, 25). In this study, the steel substrate surface was irradiated by laser beam, which heated the substrate thus softening the surface; in this case, the critical velocity could be reduced. Therefore, a lower impact velocity of 500 m/s was chosen in the simulations. The critical velocity of Cu particles deposited onto steel substrate is 800 m/s, which was reported by Zhou et al. and Huang et al. (Ref 26, 27). The typical powder particle size for CS ranges from 5 to 50 μm, and the particle size of 20 μm has been chosen for simulation analysis in many literatures (Ref 28-30). Therefore, a Cu particle size of 20 μm was selected for the simulation analysis in this study, which is also very close to the mean particle size of the Cu powder actually used in this study as shown in Fig. 1. The softening effect of Cu particle (20 μm) and steel substrate by laser irradiation was simulated by realizing the different temperatures on particle, substrate, and both.

3. Results and Discussions

3.1 Effect of Laser Irradiation on Coating Surface Morphology

The three-dimensional (3D) profiles of surface morphology of cold-sprayed Cu (CS-Cu) and supersonic laser deposition Cu (SLD-Cu) coatings are shown in Fig. 4. It can be seen that the coating surface prepared by CS (Fig. 4a) is more rugged than that by SLD (Fig. 4b). The asperities in the former are higher and holes are deeper. These differences suggest that with the assistance of laser irradiation a smoother coating surface is achievable.

Table 3 Results of surface roughness measurements for CS-Cu and SLD-Cu coatings

Sample	Measurement position	Ra, μm	Rq, μm
CS-Cu	1	23.31	27.55
	2	23.19	27.77
	3	23.36	27.62
SLD-Cu	1	18.09	22.17
	2	17.95	22.31
	3	18.14	22.26

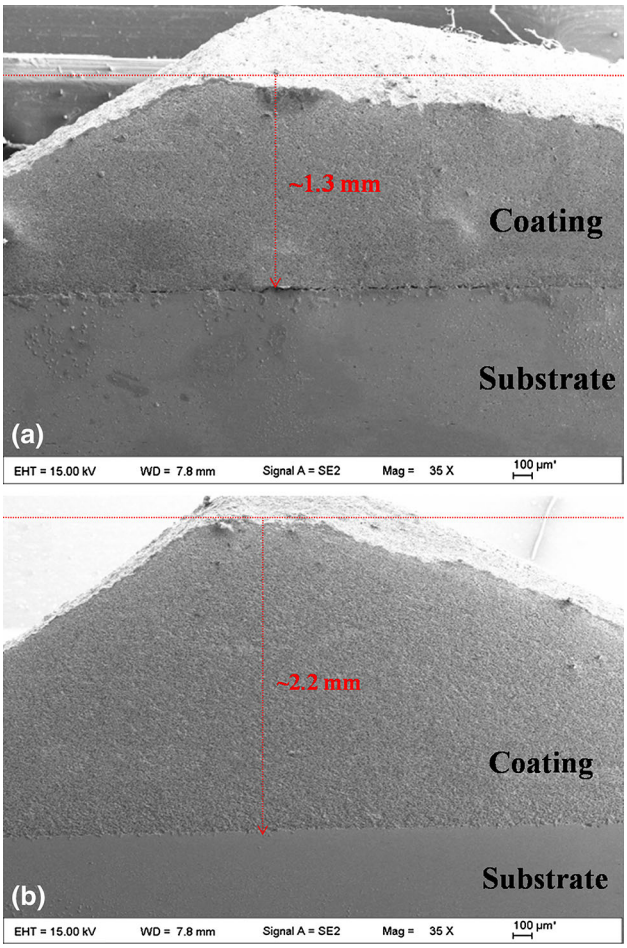

Fig. 5 Comparison of coating thickness (a) CS-Cu, (b) SLD-Cu

Table 4 The weight change of substrate and total weight of feedstock powder for each experiment

Sample	Substrate weight before deposition, g	Substrate weight after deposition, g	Total weight of feedstock powder, g
CS-Cu	171.42	182.30	40
SLD-Cu	174.19	195.33	40

In order to effectively compare the two surface morphologies of CS-Cu and SLD-Cu coatings, surface roughness measurement was performed on these specimens. Three different positions were measured on each

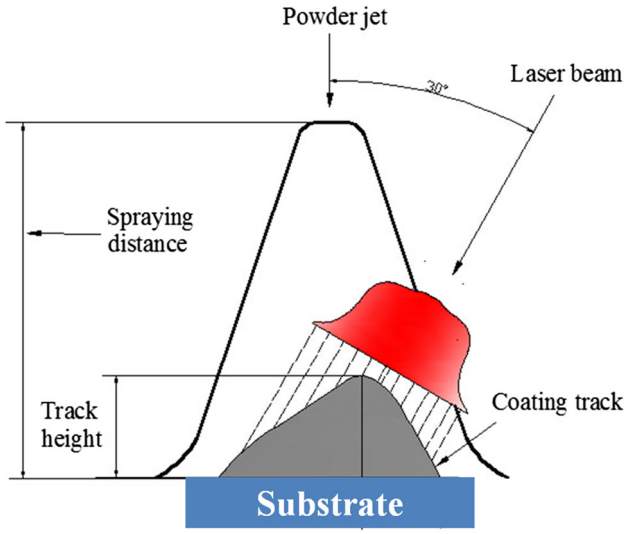

Fig. 6 Schematic demonstration of powder distribution and laser power distribution in the SLD process

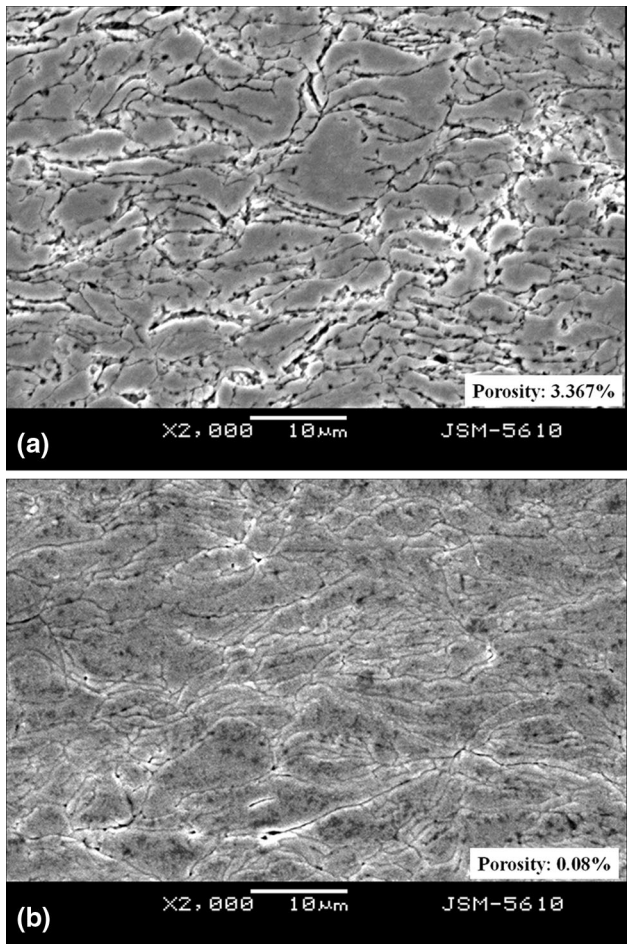

Fig. 7 Comparison of coating density (a) CS-Cu, (b) SLD-Cu

specimen. The results are presented in Table 3. It can be seen that both Ra and Rq values for SLD-Cu are lower than that for CS-Cu, which quantitatively demonstrates

the beneficial effect of laser irradiation on the coating surface quality. Similar results were reported by Danlos et al. using combined laser ablation and laser heating to modify the substrate surface morphology of CS (Ref 31). In their study, the substrate surfaces are smoother with the heating of the surface by the combination of ablation laser and heating laser. A smooth surface of SLD-Cu coating is beneficial for its post-machining.

3.2 Effect of Laser Irradiation on Coating Thickness

Figure 5 shows the comparison of coating thickness between CS-Cu and SLD-Cu coatings. It is evident that the SLD-Cu coating is thicker than the CS-Cu coating. The peak coating thickness of CS-Cu coating is about 1.3 mm (Fig. 5a), while that of SLD-Cu coating is around 2.2 mm (Fig. 5b), that is, laser irradiation increased the peak coating thickness by 70%. In other words, laser irradiation improved the deposition efficiency significantly, which is ascribed to preheating of the particles and substrate. The pyramidal morphology of the coatings shown in Fig. 5 resulted from the different velocities of the spraying particles accelerated by a Laval nozzle. Prior to hitting the substrate, the spraying particles were accelerated by a Laval nozzle as shown in Fig. 2. Due to the disturbance effect of nozzle wall, the particles close to the nozzle wall had lower velocities than the particles close to the axis of the nozzle. Particles with different impact velocities had different deposition efficiencies (viz. coating thickness). The particles close to the axis of the nozzle had high deposition efficiency and those close to the nozzle wall had low deposition efficiency. Therefore, the coatings exhibit pyramidal morphology due to the variation of particle impact velocity across the nozzle diameter.

In SLD, laser heats both the particles and substrate to the temperatures between 30 and 80% of their melting points (Ref 32), which is different from laser cladding and laser alloying where the deposition temperature is over the melting point of substrate material. Thus, thermal-affected zone in the substrate is usually negligible in the SLD process due to low heat input. In this study, the temperature of deposition site was detected as 700 °C by pyrometer, which was about 70% of the melting point of Cu and 50% of the melting point of carbon steel. The

Fig. 9 Numerical simulation of the impact of Cu particle onto carbon steel substrate (a) Cu particle: 298 K, substrate: 298 K, (b) Cu particle: 673 K, substrate: 298 K, (c) Cu particle: 298 K, substrate: 973 K, (d) Cu particle: 673 K, substrate: 973 K

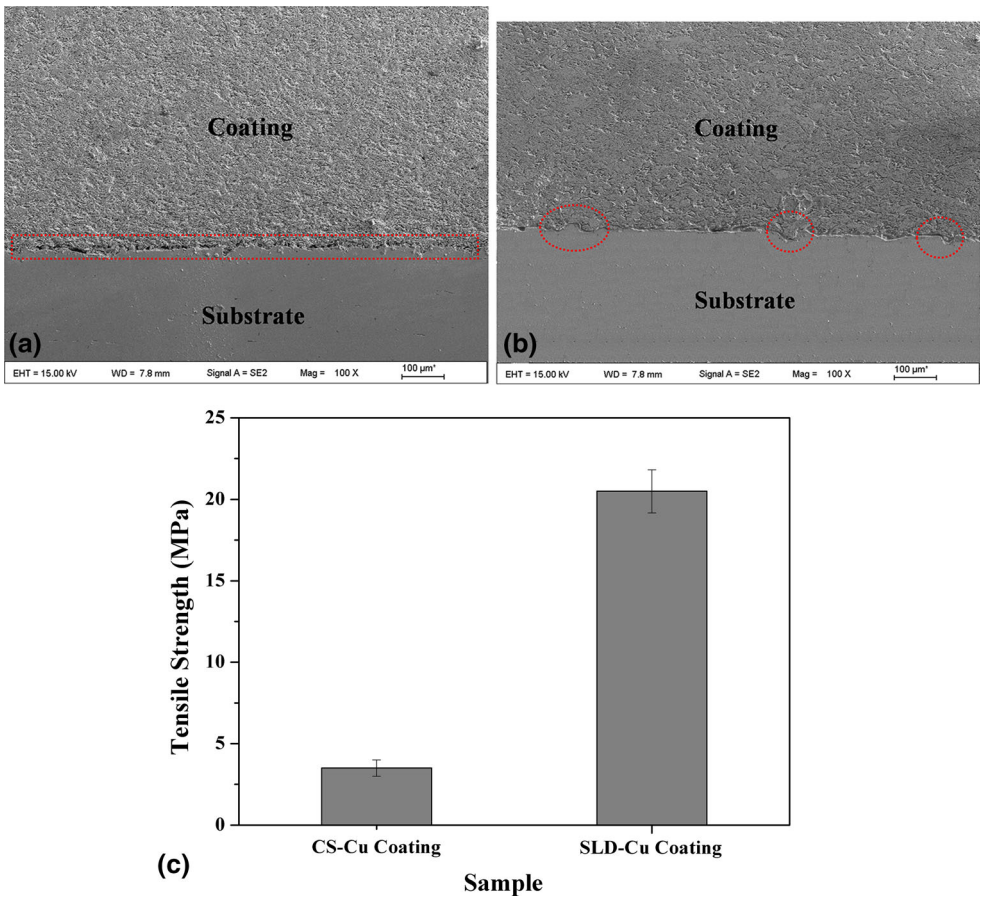

Fig. 8 Coating-substrate interfacial bonding of (a) CS-Cu coating, (b) SLD-Cu coating; and (c) the comparison of adhesion strength

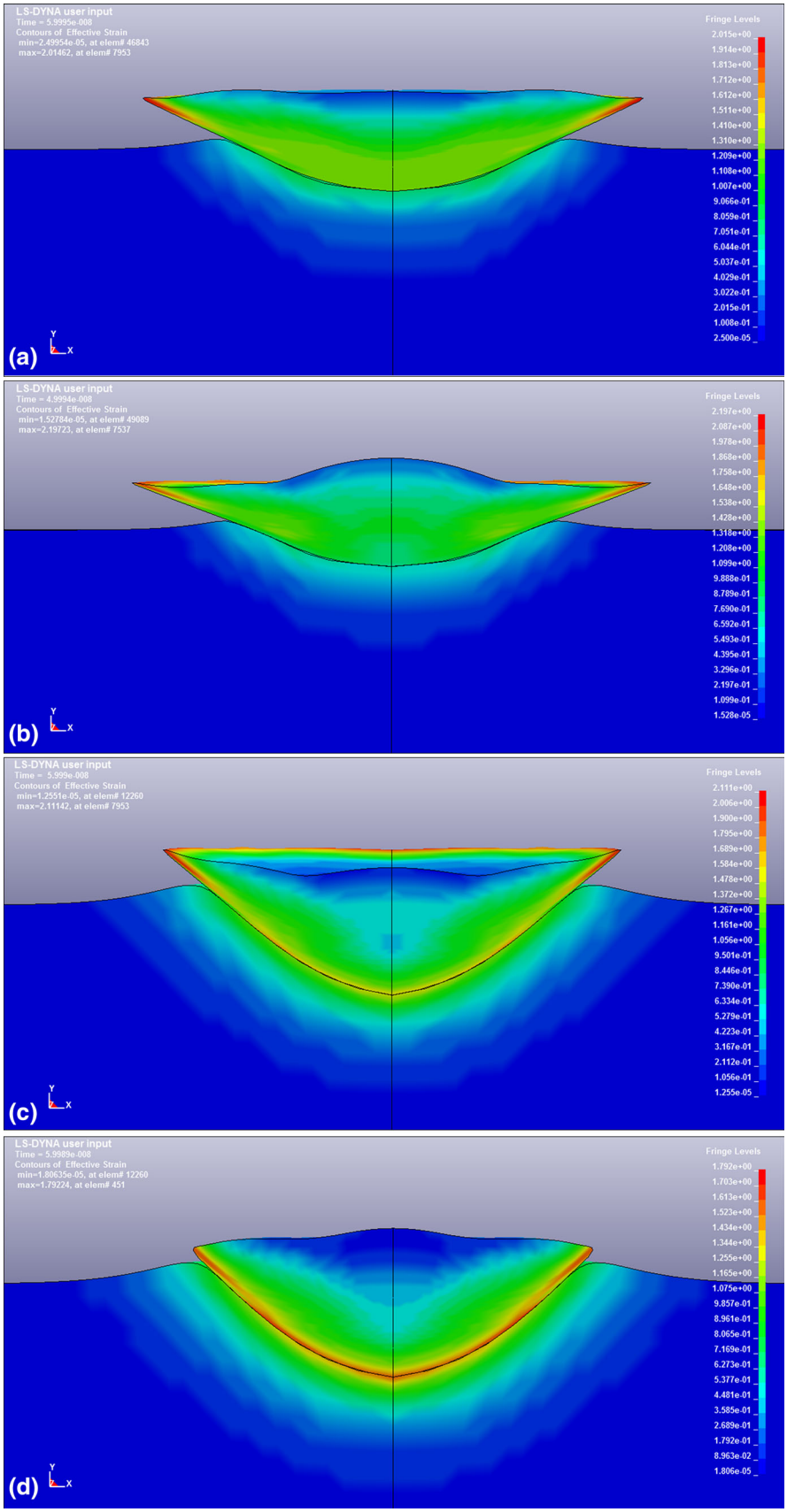

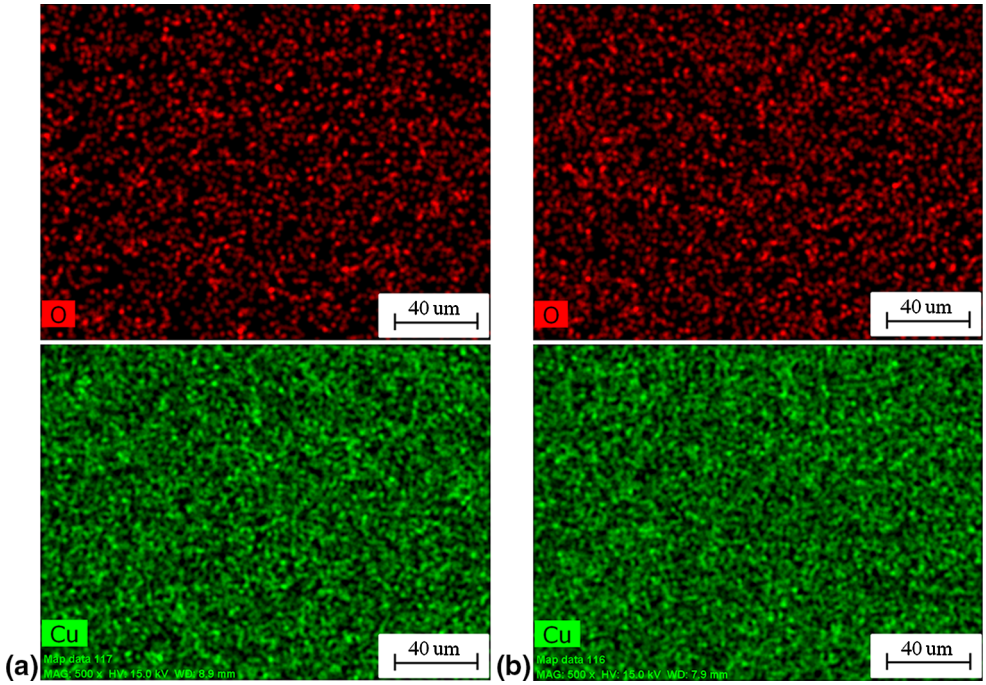

Fig.10 EDS mapping images of CS-Cu coating (a) and SLD-Cu coating (b)

spraying particle and substrate surface can be softened and lose strength at this temperature. The softer substrate surface easily accommodates deformation thus allowing the particles to be embedded to form a coating at an impact velocity about half of that in the CS process. In the meanwhile, the heated particles get easily deformed, which also benefits the adhesion to the substrate and (or) already deposited coating. Particle velocities in CS are generally distributed over a range of value due to different particle sizes as shown in Fig. 1, therefore only a fraction of particles whose velocities exceed the critical deposition velocity can participate in the coating formation. The reduction of critical deposition velocity due to laser irradiation would definitely increase the weight fraction of the particle that can be successfully deposited on the substrate. As a result, the coating thickness with laser irradiation is larger than the counterpart without laser irradiation, as demonstrated in Fig. 5.

In order to gain further insight into how much particles were bond to the substrate, deposition efficiency (DE) was calculated experimentally, which is defined as the weight of successfully bonded particles onto the substrate (M_s = final weight of the substrate − the initial substrate weight) divided by the total weight of the initial feedstock powder used (M_t) (Ref 1). The mathematical formula of deposition efficiency can be written as follows:

$$\mathrm{DE} = \frac{M_s}{M_t} \times 100\% \qquad \text{(Eq 1)}$$

The experimental data of the weight change of substrate before and after deposition are listed in Table 4, along with the total weight of the initial feedstock powder used for each experiment. The reason why the relatively large amount of powder (40 g) was used is to reduce measurement error. Before each experiment, the total weight of the initial feedstock powder (M_t) was measured by an electronic balance. Based on the data shown in Table 4, the deposition efficiency for CS-Cu and SLD-Cu coatings was calculated to be 27.2 and 52.9%, respectively. It can be seen that the deposition efficiency of cold-sprayed Cu coating was improved by about two times with the assistance of laser irradiation. However, since the laser spot is smaller than the powder footprint and the distribution of laser energy (a near top hat distribution) is non-uniform as schematically shown in Fig. 6, the deposition efficiency of SLD-Cu coating was still limited. Using a more powerful laser would enable the laser spot to be increased to the size of the powder footprint while keeping the laser power density constant, which would further improve the deposition efficiency.

3.3 Effect of Laser Irradiation on Coating Density

Figure 7 shows the SEM images of the cross-section of the CS-Cu and SLD-Cu coatings. It is observed that the cold-sprayed Cu coating contains lots of gaps and pores between the deformed Cu particles, see Fig. 7(a), while the SLD one has a much denser microstructure, with gaps and pores hardly observed, see Fig. 7(b). Porosity measurements using image analysis software indicated that the porosity of the CS-Cu coating was 3.367% in area, while it was only 0.08% in area for the SLD-Cu coating. This, again, confirms the beneficial effect of laser irradiation on coating deposition in the CS process. Furthermore, it is also interesting to notice that particle deformation in the

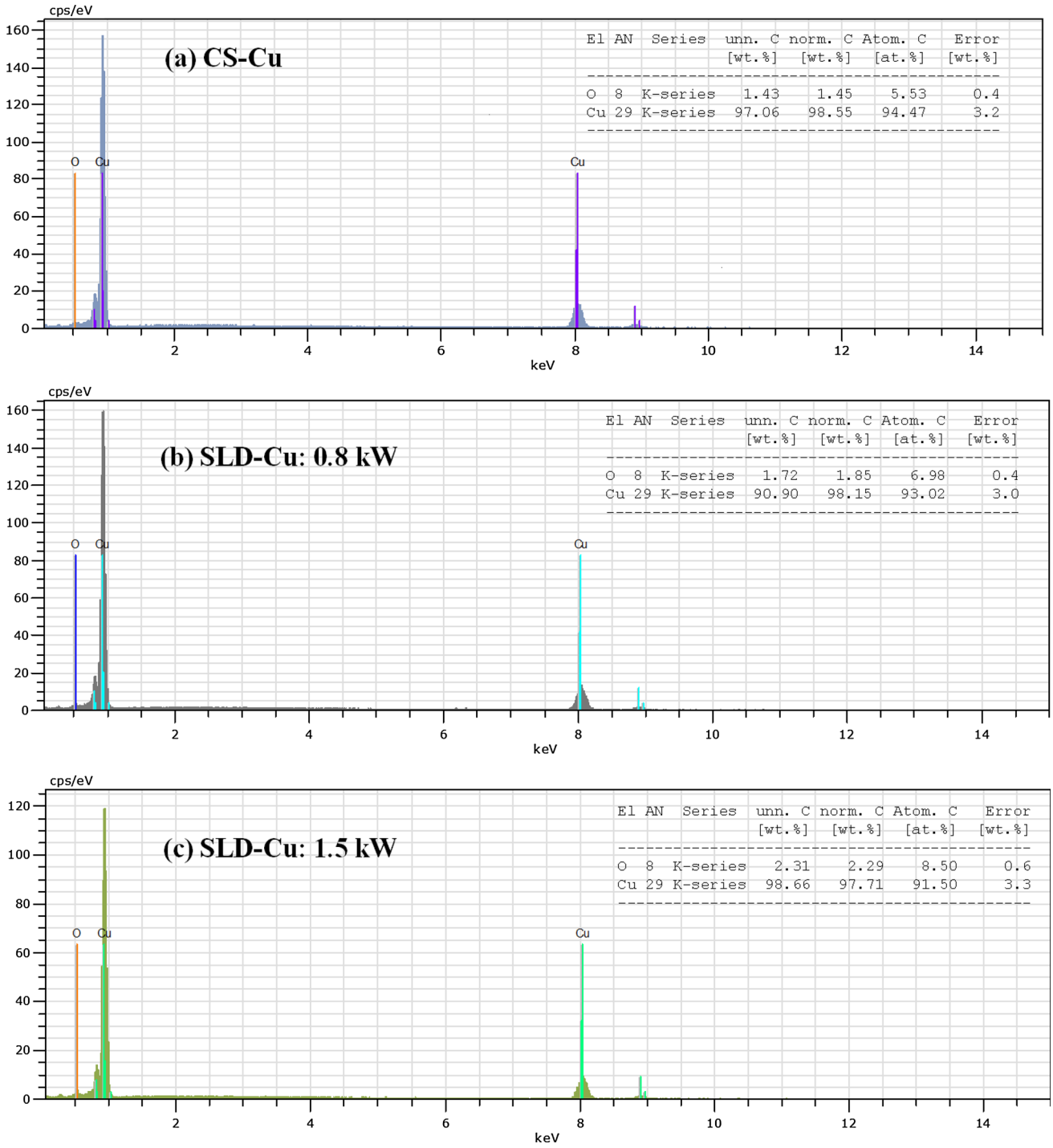

Fig. 11 The quantitative EDS results of CS-Cu and SLD-Cu coatings

SLD process is more severe than that in the CS process, as seen in Fig. 7. This is mainly due to the softening of particles by laser irradiation. In the CS process, the initially deposited particles are hammered by successive high-velocity impacting particles. The softened particles by laser heating get easily deformed by the impact of particles at a high velocity, leading to tight bonding to the substrate and/or already deposited particles. Pore-free coatings can prevent the chemical solutions from penetrating into the interior of the coatings during electrochemical test, thus more resistant to chemical degradation. The study of Kulmala et al. (Ref 33) showed that the laser-assisted low-pressure cold-sprayed copper coating had denser surface and thus higher open cell potential than the copper

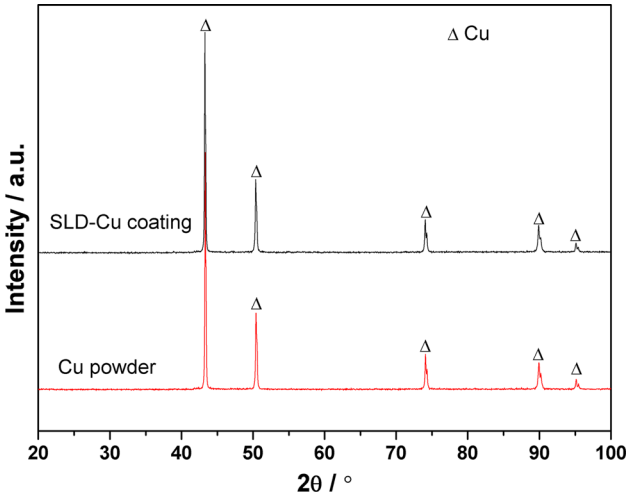

Fig.12 XRD patterns of Cu coating and Cu feedstock

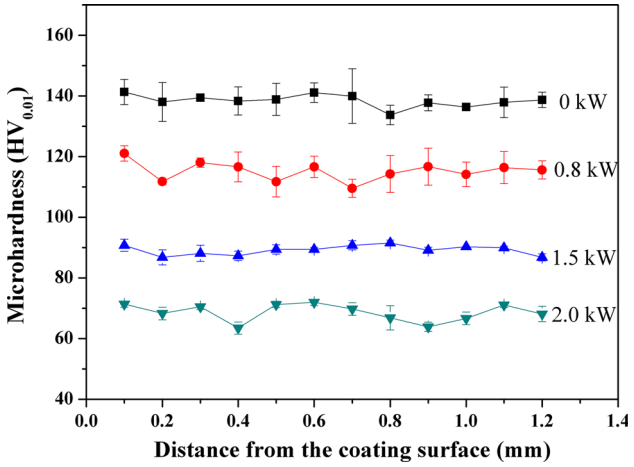

Fig.13 Microhardness of Cu coatings prepared with different laser powers

coating cold sprayed without laser assistance, indicating dense coatings are more resistant to chemical degradation.

3.4 Effect of Laser Irradiation on Interfacial Bonding

As shown in Fig. 8, laser irradiation also plays an important role in coating/substrate interfacial bonding. There is an obvious crack observed at the interface between coating layer and substrate of the CS-Cu coating specimen, as marked in Fig. 8(a), but this is not found in the SLD-Cu coating specimen, instead, material penetration has occurred at the interface of this coating, as marked in Fig. 8(b), which enhances the coating bonding to the substrate. In order to quantify the real bonding force for each coating, adhesion strength test as described in the ASTM Standard C633 was performed on the CS-Cu and SLD-Cu coatings. The test included coating one surface of a substrate fixture with a circular area (10 mm diameter), bonding this coating to the surface of a loading fixture with an epoxy resin adhesive, and then applying a tensile load normal to the plane of the coating. The comparison of adhesion strength of CS-Cu and SLD-Cu coatings is shown in Fig. 8(c). It can be seen that the adhesion strength of the CS-Cu coating is very weak but it increased significantly with the assistance of laser irradiation.

Currently, the most widely accepted bonding mechanism of CS is the occurrence of adiabatic shear instability at the interface, which results from the high strain rate and the intensive localized deformation during the particle deposition process (Ref 19, 34). The interfacial instability occurring during the high-velocity impacting process results in material roll-ups and vortices at the interface, as a consequence, substrate, and coating materials merge at the interface region, leading to mechanical interlocking (Ref 35). Another proposed bonding mechanism of CS is the metallurgical bonding by atomic diffusion between the coating and the substrate materials, which can provide better bonding strength compared to mechanical interlocking (Ref 36). However, in CS the solid-state diffusion is not sufficient to form a thick diffusion layer due to the extremely short timescale of the particle-substrate interaction and low temperature (Ref 19). In the case of synchronous laser irradiation on the deposition site, the substrate temperature is increased and it is thereby softened. The softened substrate easily lodges the particles to form mechanical interlocking. Moreover, the increased substrate temperature can promote the atomic diffusion between the coating and the substrate materials, which greatly increases the possibility of metallurgical bonding. All these contribute to the good interfacial bonding of the SLD coating.

In order to further elucidate the effect of particle and substrate softening (heated by synchronous laser irradiation) on the particle/substrate deformation behavior, the impact of Cu particle onto carbon steel substrate was numerically simulated as shown in Fig. 9. As for the particle softening (Fig. 9b), the substrate crater depth kept almost unchanged and the flattening ratio of the Cu particle increased as compared to the counterpart without particle preheating (Fig. 9a). The contact area between the particle and the substrate was limited. As for the substrate softening (Fig. 9c), the substrate crater depth increased and the Cu particle penetrated into substrate, which increased the contact area between the particle and the substrate. In the case of softening both the particle and the substrate (Fig. 9d), the substrate crater depth increased further and the Cu particle penetration into substrate was deeper. These results were in good agreement with that reported by Yu et al. (Ref 28), i.e., preheating both particle and substrate presents a coordinated deformation pattern, and the coordinated deformation pattern was transferred to be a penetration way for preheating the substrate and a spreading way for preheating the particle, respectively. In this study, the introduction of synchronous laser irradiation into CS softened both the Cu particles and the carbon steel substrate, which corresponded to the

simulation model in Fig. 9(d). The relatively large contact area between particles and substrate is beneficial to the particle deposition and the bonding between particle and substrate, which was confirmed by the experimental result as shown in Fig. 8(b).

3.5 Influence of Laser Irradiation on Coating Oxidation

The influence of laser irradiation on the coating oxidation was investigated using the EDS and XRD. The EDS results for the SLD coating are presented in Fig. 10 and 11. As can be seen from the EDS results, O element was detected for both CS-Cu and SLD-Cu coatings. The content of O element was 1.45 wt.% in the CS-Cu coating, while it was gradually increased with laser power. Since the deposition temperature of CS-Cu coating was ambient temperature, the presence of O element in this specimen implies that the feedstock powder might be initially oxidized by preheated working gas (air) prior to the production of the coating. The increased content of O element in the SLD-Cu coating may be caused by the reaction of preheated Cu powder with surrounding air when laser irradiation was employed. However, further XRD analysis (Fig. 12) on the SLD-Cu coating and Cu powder reveals that both the Cu coating and Cu feedstock are composed of Cu element but not CuO. The reason for the inconsistent results between EDS and XRD may be due to the very small amount of CuO in the coating, which cannot be detected by XRD because of the limited resolution. It should be pointed out that the slight Cu oxidation can be avoided by substituting air with N_2 as working gas.

3.6 Influence of Laser Irradiation on Coating Hardness

Shown in Fig. 13 are the microhardness of the Cu coatings deposited under different laser powers. Due to the strain-hardening effect during high-velocity impact in CS process, the microhardness of the CS-Cu coating reached 140 $HV_{0.01}$. However, with synchronous laser irradiation, the microhardness of the as-deposited coatings decreased gradually with increasing laser power. The microhardness of the SLD-Cu coating prepared with 2.0 kW laser power was only about 70 $HV_{0.01}$, which was half of that for CS-Cu coating. Therefore, it can be concluded that synchronous laser irradiation has a softening effect on the as-deposited coatings, which is similar to annealing treatment for cold-sprayed coatings (Ref 37, 38). As the microhardness of the as-sprayed coating can be optimized through annealing treatment, it is therefore expected that the cohesion strength of the as-sprayed coating could be improved through the healing up of the weakly bonded particle interfaces by synchronous laser irradiation, which resulted in high coating density as shown in Fig. 7. However, it should be noted that the laser power should be not too high, in order to avoid coating oxidation and substrate melting.

4. Conclusions

The effects of synchronous laser irradiation on the cold-sprayed Cu coating were investigated. The coating surface morphology, thickness, density, interfacial bonding, oxidation, and coating microhardness were analyzed with various technologies such as SEM, EDS, XRD, and 3D profilometer.

3D surface profiles reveal that the coating surface of SLD-Cu is smoother than that of CS-Cu, which is beneficial for post-machining. The deposition efficiency measurements show that the deposition efficiency of cold-sprayed Cu powder is improved significantly by synchronous laser irradiation due to the reduction of critical particle velocity.

The density of the CS-Cu coating can be improved by laser irradiation, because the heated particles easily deform thus producing intimate bonding between particles. Moreover, synchronous laser irradiation enhances the interfacial bonding between the coating and the substrate. The microhardness of the as-deposited coatings decreased with the introduction of laser irradiation. The EDS and XRD analyses find oxidation occurrence in the SLD coating, but the oxide is trivial. The obtained results demonstrate that SLD is capable of producing coatings with high efficiency, good quality, and trivial oxidation.

Acknowledgments

The authors would like to appreciate financial supports from Major Scientific and Technological Special Key Industrial Project of Zhejiang Province (2012C11001), National Natural Science Foundation of China (Grant No. 51475429), Youth Foundation Project of Natural Science Foundation of Zhejiang Province (LQ13E050012), Commonweal Technology Research Industrial Project of Zhejiang Province (2013C31012), and Postdoctoral Scientific Research Project of Zhejiang Province (Z42102 002). The authors also would like to specially appreciate Prof. Rong Liu from Carleton University for her kind help in article modification.

References

1. A. Papyrin, V. Kosarev, K.V. Klinkov, and V.M. Fomin, *Cold Spray Technology*, Elsevier Ltd., Oxford, 2006
2. V.K. Champagne, *The Cold Spray Materials Deposition Process: Fundamentals and applications*, Woodhead Publishing Ltd, Cambridge, 2007
3. R.G. Maev and V. Leshchynsky, *Introduction to Low Pressure Gas Dynamic Spray*, Wiley, New York, 2008
4. W. Wong, P. Vo, E. Irissou, A.N. Ryabinin, J.G. Legoux, and S. Yue, Effect of Particle Morphology and Size Distribution on Cold-Sprayed Pure Titanium Coatings, *J. Therm. Spray Technol.*, 2013, **22**(7), p 1140-1153
5. T. Suhonen, T. Varis, S. Dosta, M. Torrell, and J.M. Guilemany, Residual Stress Development in Cold Sprayed Al, Cu and Ti Coatings, *Acta Mater.*, 2013, **61**, p 6329-6337
6. B. AL-Mangour, R. Mongrain, E. Irissou, and S. Yue, Improving the Strength and Corrosion Resistance of 316L Stainless Steel for

Biomedical Applications Using Cold Spray, *Surf. Coat. Technol.*, 2013, **216**, p 297-307
7. Q. Zhang, C.J. Li, X.R. Wang, Z.L. Ren, C.X. Li, and G.J. Yang, Formation of NiAl Intermetallic Compound by Cold Spraying of Ball-Milled Ni/Al Alloy Powder Through Postannealing Treatment, *J. Thermal. Spray Technol.*, 2008, **17**(5–6), p 715-720
8. A.S. Alhulaifi, G.A. Buck, and W.J. Arbegast, Numerical and Experimental Investigation of Cold Spray Gas Dynamic Effects for Polymer Coating, *J. Therm. Spray Technol.*, 2012, **21**(5), p 852-862
9. M. Gardon, A. Latorre, M. Torrell, S. Dosta, J. Fernandez, and J.M. Guilemany, Cold Gas Spray Titanium Coatings onto A Biocompatible Polymer, *Mater. Lett.*, 2013, **106**, p 97-99
10. S. Kikuchi, S. Yoshino, M. Yamada, M. Fukumoto, and K. Okamoto, Microstructures and Thermal Properties of Cold-Sprayed Cu-Cr Composite Coatings, *J. Therm. Spray Technol.*, 2013, **22**(6), p 926-931
11. X.T. Luo, G.J. Yang, C.J. Li, and K. Kondoh, High Strain Rate Induced Localized Amorphization in Cubic BN/NiCrAl Nanocomposite Through High Velocity Impact, *Scripta Mater.*, 2011, **65**, p 581-584
12. W.Y. Li, M. Yu, F.F. Wang, S. Yin, and H.L. Liao, A Generalized Critical Velocity Window Based on Material Property for Cold Spray by Eulerian Method, *J. Thermal. Spray Technol.*, 2014, **23**(3), p 557-566
13. T. Schmidt, F. Gaertner, and H. Kreye, New Development in Cold Spray Based on Higher Gas and Particle Temperatures, *J. Thermal. Spray Technol.*, 2006, **15**(4), p 488-494
14. T. Schmidt, H. Assadi, F. Gartner, H. Richter, T. Stoltenhoff, H. Kreye, and T. Klassen, From Particle Acceleration to Impact and Bonding in Cold Spraying, *J. Thermal. Spray Technol.*, 2009, **18**(5–6), p 794-808
15. W.Y. Li and C.J. Li, Optimal design of a Novel Cold Spray Gun Nozzle at a limited Space, *J. Thermal. Spray Technol.*, 2005, **14**(3), p 391-396
16. M. Fukumoto, H. Wada, K. Tanabe, M. Yamada, E. Yamaguchi, A. Niwa, M. Sugimoto, and M. Izawa, Effect of Substrate Temperature on Deposition Behavior of Copper Particles on Substrate Surfaces in the Cold Spray Process, *J. Thermal. Spray Technol.*, 2007, **16**(5–6), p 643-650
17. J.G. Legoux, E. Irissou, and C. Moreau, Effect of Substrate Temperature on the Formation Mechanism of Cold-Sprayed Aluminum, Zinc and Tin Coatings, *J. Thermal. Spray Technol.*, 2007, **16**(5–6), p 619-626
18. P.C. King, G. Bae, S.H. Zahiri, M. Jahedi, and C. Lee, An Experimental and Finite Element Study of Cold Spray Copper Impact onto Two Aluminum Substrates, *J. Thermal. Spray Technol.*, 2010, **19**(3), p 620-634
19. H. Assadi, F. Gartner, T. Stoltenhoff, and H. Kreye, Bonding Mechanism in Cold Gas Spraying, *Acta Mater.*, 2003, **51**, p 4379-4394
20. J.H. Lee et al., *Effect of Particle Temperature on the Critical Velocity for Particle Deposition by Kinetic Spraying, ITSC2006: International Thermal Spray Conference*, Seattle, USA, 2006
21. M. Bray, A. Cockburn, and W. O'Neill, The Laser-assisted Cold Spray Process and Deposit Characterisation, *Surf. Coat. Technol.*, 2009, **203**, p 2851-2857
22. F. Luo, A. Cockburn, R. Lupoi, M. Sparkes, and W. O'Neill, Performance Comparison of Stellite 6 Deposited on Steel Using Supersonic Laser Deposition and Laser Cladding, *Surf. Coat. Technol.*, 2012, **212**, p 119-127
23. W.Y. Li, H.L. Liao, C.J. Li, H.S. Bang, and C. Coddet, Numerical Simulation of Deformation Behavior of Al Particles Impacting on Al Substrate and Effect of Surface Oxide Films on Interfacial Bonding in Cold Spray, *Appl. Surf. Sci.*, 2007, **253**(11), p 5084-5091
24. W.Y. Li, H.L. Liao, C.J. Li, G. Li, C. Coddet, and X.F. Wang, On High Velocity Impact of Micro-Sized Metallic Particles in Cold Spraying, *Appl. Surf. Sci.*, 2006, **253**, p 2852-2862
25. G. Bae, Y.M. Xiong, S. Kumar, K. Kang, and C.H. Lee, General Aspects of Interface Bonding in Kinetic Sprayed Coatings, *Acta Mater.*, 2008, **56**(17), p 4858-4868
26. H.H. Guo, X.L. Zhou, X.K. Wu, H. Cui, J.C. Liu, and J.S. Zhang, Preparation and Simulation of Cold Sprayed Copper Coatings on Metal Substrate, *Trans. Mater. Heat Treat.*, 2009, **30**(6), p 158-163
27. R.Z. Huang, W.H. Ma, and H. Fukanuma, Development of Ultra-strong Adhesive Strength Coatings Using Cold Spray, *Surf. Coat. Technol.*, 2014, **258**, p 832-841
28. M. Yu, W.Y. Li, F.F. Wang, X.K. Suo, and H.L. Liao, Effect of Particle and Substrate Preheating on Particle Deformation Behavior in Cold Spray, *Surf. Coat. Technol.*, 2013, **220**, p 174-178
29. S. Yin, X.F. Wang, X.K. Suo, H.L. Liao, Z.W. Guo, W.Y. Li, and C. Coddet, Deposition Behavior of Thermally Softened Copper Particles in Cold Spraying, *Acta Mater.*, 2013, **61**, p 5105-5118
30. M. Yu, W.Y. Li, F.F. Wang, and H.L. Liao, Finite Element Simulation of Impacting Behavior of Particles in Cold Spraying by Eulerian Approach, *J. Thermal. Spray Technol.*, 2012, **21**, p 745-752
31. Y. Danlos, S. Costil, X. Guo, H. Liao, and C. Coddet, Ablation Laser and Heating Laser Combined to Cold Spraying, *Surf. Coat. Technol.*, 2010, **205**, p 1055-1059
32. E.O. Olakanmi and M. Doyoyo, Laser-Assisted Cold-Sprayed Corrosion- and Wear-Resistant Coatings: A Review, *J. Thermal. Spray Technol.*, 2014, **23**(5), p 765-785
33. M. Kulmala and P. Vuoristo, Influence of Process Conditions in Laser-assisted Low-pressure Cold Spraying, *Surf. Coat. Technol.*, 2008, **202**, p 4503-4508
34. M. Grujicic, C.L. Zhao, W.S. DeRosset, and D. Helfritch, Adiabatic Shear Instability Based Mechanism for Particle/Substrate Bonding in the Cold-Gas Dynamic-Spray Process, *Mater. Des.*, 2004, **25**(8), p 681-688
35. M. Grujicic, J.R. Saylor, D.E. Beasley, W.S. DeRosset, and D. Helfritch, Computational Analysis of the Interfacial Bonding Between Feed-Powder Particles and the Substrate in the Cold-Gas Dynamic-Spray Process, *Appl. Surf. Sci.*, 2003, **219**, p 211-227
36. C.J. Li, W.Y. Li, and Y.Y. Wang, Formation of Metastable Phases in Cold-Sprayed Soft Metallic Deposit, *Surf. Coat. Technol.*, 2005, **198**, p 469-473
37. X.M. Meng, J.B. Zhang, W. Han, J. Zhao, and Y.L. Liang, Influence of Annealing Treatment on the Microstructure and Mechanical Performance of Cold Sprayed 304 Stainless Steel Coating, *Appl. Surf. Sci.*, 2011, **258**, p 700-704
38. E. Calla, D.G. McCartney, and P.H. Shipway, Effect of Deposition Conditions on the Properties and Annealing Behavior of Cold-Sprayed Copper, *J. Thermal. Spray Technol.*, 2006, **15**(2), p 255-262